

## Charmless $B_s^0$ decays at Belle

---

**Bilas Pal**\*†

*University of Cincinnati*

*E-mail:* [palbs@ucmail.uc.edu](mailto:palbs@ucmail.uc.edu)

We report on recent results on charmless hadronic and radiative rare  $B_s^0$  decays, based on the data collected by the Belle experiment at the KEKB  $e^+e^-$  collider. These include the studies of  $B_s^0 \rightarrow K^0 \bar{K}^0$ ,  $B_s^0 \rightarrow \phi \gamma$  and  $B_s^0 \rightarrow \gamma \gamma$ .

*XIII International Conference on Heavy Quarks and Leptons*

*22-27 May, 2016*

*Blacksburg, Virginia, USA*

---

\*Speaker.

†On behalf of the Belle Collaboration

## 1. Introduction

Charmless hadronic  $B$  decays are suppressed compared to other hadronic  $B$  decays and hence can be excellent probes for new physics beyond the Standard Model (SM). In this paper, we present recent results from the Belle experiment on the charmless hadronic and radiative  $B_s^0$  decays  $B_s^0 \rightarrow K^0 \bar{K}^0$ ,  $B_s^0 \rightarrow \phi \gamma$  and  $B_s^0 \rightarrow \gamma \gamma$ .

The main challenge of studying the charmless  $B_s^0$  decays is the suppression of overwhelmingly large background arising from continuum  $e^+e^- \rightarrow q\bar{q}$  ( $q = u, d, c, s$ ) production. To suppress this background, we use a multivariate analyzer based on a neural network. The neural network uses the so-called event shape variables to discriminate continuum events, which tend to be jetlike, from spherical  $B\bar{B}$  events. Signal decays are identified by two kinematical variables: the beam-energy-constrained mass  $M_{bc} = \sqrt{E_{\text{beam}}^2 - |\vec{p}_B|^2 c^2/c^2}$  and the energy difference  $\Delta E = E_B - E_{\text{beam}}$ . To determine the signal yield, normally an unbinned extended maximum likelihood fit is applied to all candidate event using the above two kinematical variables and other useful information. The signal probability density functions (PDF) of these two variables are typically studied from Monte Carlo (MC) simulation and the background PDF can be obtained either from MC simulation or sideband data. A high statistics control sample of similar topology is used to understand potential data/MC differences.

## 2. Observation of the decay $B_s^0 \rightarrow K^0 \bar{K}^0$

The two-body decays  $B_s^0 \rightarrow h^+ h'^-$ , where  $h^{(0)}$  is either a pion or kaon, have now all been observed [1]. In contrast, the neutral-daughter decays  $B_s^0 \rightarrow h^0 h'^0$  have yet to be observed. The decay  $B_s^0 \rightarrow K^0 \bar{K}^0$  [2] is of particular interest because the branching fraction is predicted to be relatively large. In the SM, the decay proceeds mainly via a  $b \rightarrow s$  loop (or ‘‘penguin’’) transition as shown in Fig. 1, and the branching fraction is predicted to be in the range  $(16 - 27) \times 10^{-6}$  [3]. The presence of non-SM particles or couplings could enhance this value [4]. It has been pointed out that  $CP$  asymmetries in  $B_s^0 \rightarrow K^0 \bar{K}^0$  decays are promising observables to search for new physics [5].

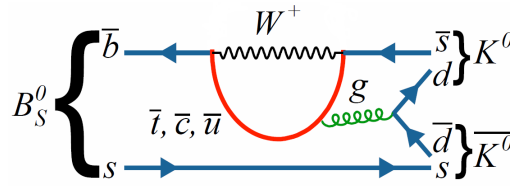


**Figure 1:** Loop diagram for  $B_s^0 \rightarrow K^0 \bar{K}^0$  decays.

The current upper limit on the branching fraction,  $\mathcal{B}(B_s^0 \rightarrow K^0 \bar{K}^0) < 6.6 \times 10^{-5}$  at 90% confidence level (C.L.), was set by the Belle Collaboration using  $23.6 \text{ fb}^{-1}$  of data recorded at the  $\Upsilon(5S)$  resonance [6]. The analysis presented here uses the full data set of  $121.4 \text{ fb}^{-1}$  recorded at the  $\Upsilon(5S)$ . Improved tracking,  $K^0$  reconstruction and continuum suppression algorithms are also used in this analysis. The data set corresponds to  $(6.53 \pm 0.66) \times 10^6 B_s^0 \bar{B}_s^0$  pairs [7] produced in three  $\Upsilon(5S)$  decay channels:  $B_s^0 \bar{B}_s^0$ ,  $B_s^{*0} \bar{B}_s^0$  or  $B_s^0 \bar{B}_s^{*0}$ , and  $B_s^{*0} \bar{B}_s^{*0}$ . The latter two channels dominate,

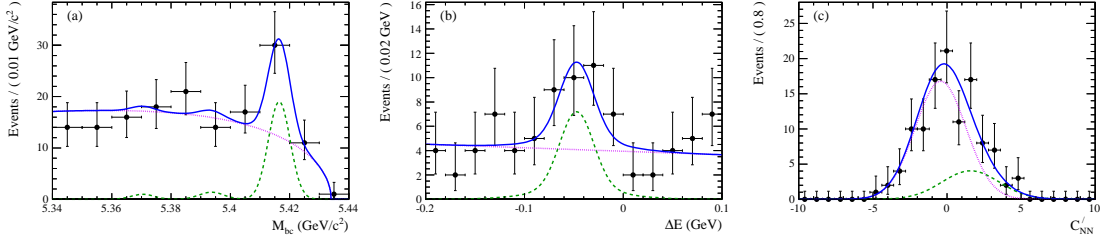


**Figure 2:** Projections of the 3D fit to the real data: (a)  $M_{bc}$  in  $-0.11 \text{ GeV} < \Delta E < 0.02 \text{ GeV}$  and  $C'_{NN} > 0.5$ ; (b)  $\Delta E$  in  $5.405 \text{ GeV}/c^2 < M_{bc} < 5.427 \text{ GeV}/c^2$  and  $C'_{NN} > 0.5$ ; and (c)  $C'_{NN}$  in  $5.405 \text{ GeV}/c^2 < M_{bc} < 5.427 \text{ GeV}/c^2$  and  $-0.11 \text{ GeV} < \Delta E < 0.02 \text{ GeV}$ . The points with error bars are data, the (green) dashed curves show the signal, (magenta) dotted curves show the continuum background, and (blue) solid curves show the total. The three peaks in  $M_{bc}$  arise from  $\Upsilon(5S) \rightarrow B_s^0 \bar{B}_s^0, B_s^{*0} \bar{B}_s^0 + B_s^0 \bar{B}_s^{*0}$ , and  $B_s^{*0} \bar{B}_s^{*0}$  decays.

with production fractions of  $f_{B_s^{*0} \bar{B}_s^0} = (7.3 \pm 1.4)\%$  and  $f_{B_s^0 \bar{B}_s^0} = (87.0 \pm 1.7)\%$  [8]. The  $B_s^{*0}$  decays via  $B_s^{*0} \rightarrow B_s^0 \gamma$ , and the  $\gamma$  is not reconstructed.

Candidate  $K^0$  mesons are reconstructed via the decay  $K_S^0 \rightarrow \pi^+ \pi^-$  and require that the  $\pi^+ \pi^-$  invariant mass be within  $12 \text{ MeV}/c^2$  of the nominal  $K_S^0$  mass [1]. In order to extract the signal yield, we perform a three-dimensional (3D) unbinned maximum likelihood fit to the variables,  $M_{bc}$ ,  $\Delta E$ , and continuum suppression variable  $C'_{NN} = \ln \left( \frac{C_{NN} - C_{NN}^{\min}}{C_{NN}^{\max} - C_{NN}} \right)$ . We extract  $29.0^{+8.5}_{-7.6}$  signal events and  $1095.0^{+33.9}_{-33.4}$  continuum background events. Projections of the fit are shown in Fig. 2. The branching fraction of the decay  $B_s^0 \rightarrow K^0 \bar{K}^0$  is measured to be [9]

$$\mathcal{B}(B_s^0 \rightarrow K^0 \bar{K}^0) = (19.6^{+5.8}_{-5.1} \pm 1.0 \pm 2.0) \times 10^{-6}, \quad (2.1)$$

where the first uncertainty is statistical, the second is systematic, and the third reflects the uncertainty due to the total number of  $B_s^0 \bar{B}_s^0$  pairs. The significance of this result is 5.1 standard deviations, thus, our measurement constitutes the first observation of this decay. This measured branching fraction is in good agreement with the SM predictions [3], and it implies that the Belle II experiment [10] will reconstruct over 1000 of these decays. Such a sample would allow for a much higher sensitivity search for new physics in this  $b \rightarrow s$  penguin-dominated decay.

### 3. Radiative $B_s^0$ decays

In the SM, the decays  $B_s^0 \rightarrow \gamma\gamma$  and  $B_s^0 \rightarrow \phi\gamma$  are explained by the radiative transitions  $b \rightarrow s\gamma\gamma$  and  $b \rightarrow s\gamma$ , respectively. The leading-order Feynman diagrams for these processes are shown in Fig. 3. First observation of the decay  $B_s^0 \rightarrow \phi\gamma$  was made by the Belle Collaboration using  $23.6 \text{ fb}^{-1}$  of data collected at the  $\Upsilon(5S)$  resonance and its branching fraction was measured to be  $(5.7^{+2.2}_{-1.9}) \times 10^{-5}$  [11]. The decay  $B_s^0 \rightarrow \gamma\gamma$ , on the other hand, has not been observed yet and the current upper limit on the branching fraction is  $8.7 \times 10^{-6}$  at 90% C.L. [11]. This is almost an order of magnitude larger than the range covered by the published theoretical calculations [12]. New physics could enhance its branching fraction by more than an order of magnitude [13].

The results presented here are based on  $121.4 \text{ fb}^{-1}$  recorded at the  $\Upsilon(5S)$ . Candidate  $\phi$  mesons are reconstructed via the decay  $\phi \rightarrow K^+ K^-$  and require that the  $K^+ K^-$  invariant mass be within  $12 \text{ MeV}/c^2$  of the nominal  $\phi$  mass [1]. For  $B_s^0 \rightarrow \phi\gamma$  ( $B_s^0 \rightarrow \gamma\gamma$ ) decay, we perform a four-dimensional

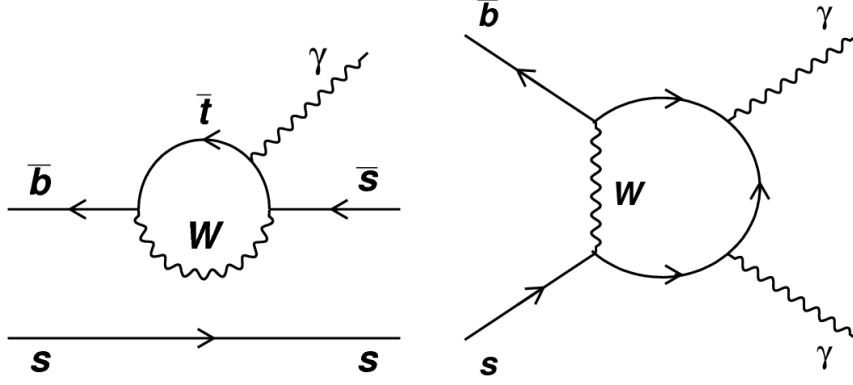


**Figure 3:** Leading-order Feynman diagrams for decays (left)  $B_s^0 \rightarrow \phi\gamma$  and (right)  $B_s^0 \rightarrow \gamma\gamma$ .

(two-dimensional) unbinned maximum likelihood fit to the variables  $M_{bc}$ ,  $\Delta E$ ,  $C'_{NB}$ <sup>1</sup> and  $\cos\theta_{\text{hel}}$  ( $M_{bc}$  and  $\Delta E$ ). The helicity angle  $\theta_{\text{hel}}$  is the angle between the  $B_s^0$  and the  $K^+$  evaluated in the  $\phi$  rest frame.

We observe  $91_{-13}^{+14}$  signal events in the  $B_s^0 \rightarrow \phi\gamma$  mode and the corresponding branching fraction is measured to be [14]

$$\mathcal{B}(B_s^0 \rightarrow \phi\gamma) = (36 \pm 5 \pm 3 \pm 6) \times 10^{-6}, \quad (3.1)$$

where the first uncertainty is statistical, the second is systematic, and the third reflects the uncertainty due to the fraction of  $B_s^{(*)}\bar{B}_s^{(*)}$  in  $b\bar{b}$  events. Fit projections are shown in Fig. 4. This improved result supersedes our earlier measurement [11] and is consistent with the recent LHCb's measurement [15].

We see no significant signal in the  $B_s^0 \rightarrow \gamma\gamma$  mode and we extract an upper limit at 90% C.L. of [14]

$$\mathcal{B}(B_s^0 \rightarrow \gamma\gamma) < 3.1 \times 10^{-6}. \quad (3.2)$$

This result represent an improvement by a factor of about 3 over the previous best measurement [11]. Fit projections are shown in Fig. 5.

## 4. Conclusions

Using the full set of Belle data collected at  $\Upsilon(5S)$  resonance, recent measurements of charmless hadronic and radiative  $B_s^0$  decays are presented. Our measurement of  $B_s^0 \rightarrow K^0\bar{K}^0$  branching fraction constitutes the first observation of the decay. This is the first observation of a charmless  $B_s^0$  decay involving only neutral hadrons.

<sup>1</sup>The definition of  $C'_{NB}$  is same as  $C'_{NN}$  as used in the previous section.

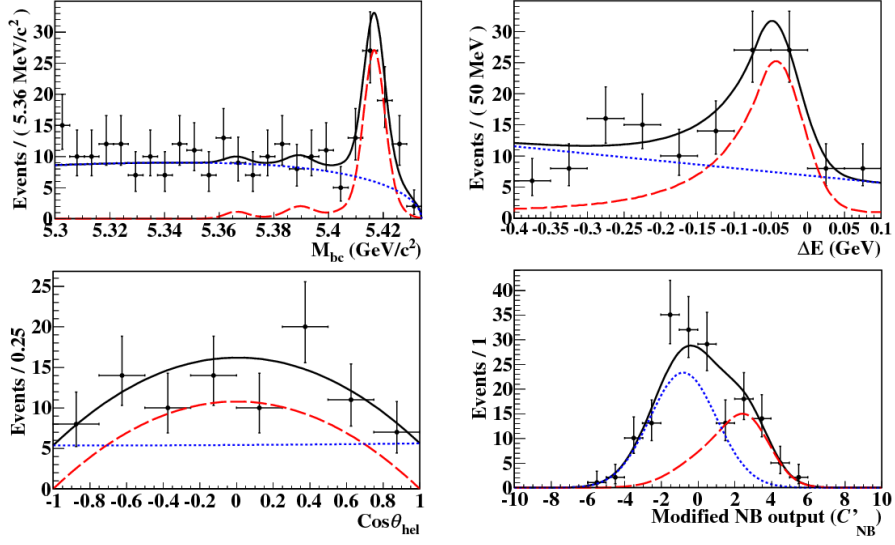


**Figure 4:** Data fits for the  $B_s^0 \rightarrow \phi\gamma$  analysis. The projections are shown only for events inside the  $B_s^*\bar{B}_s^*$  signal region except for the plotted variable. The  $B_s^*\bar{B}_s^*$  signal region is defined as  $M_{bc} > 5.4 \text{ GeV}/c^2$ ,  $-0.2 \text{ GeV} < \Delta E < 0.02 \text{ GeV}$ ,  $|\cos\theta_{\text{hel}}| < 0.8$  and  $0.0 < C'_{\text{NB}} < 10.0$ . The points with error bars represent the data, the solid black curve represents the total fit function, the red dashed (blue dotted) curve represents the signal (continuum background) contribution.

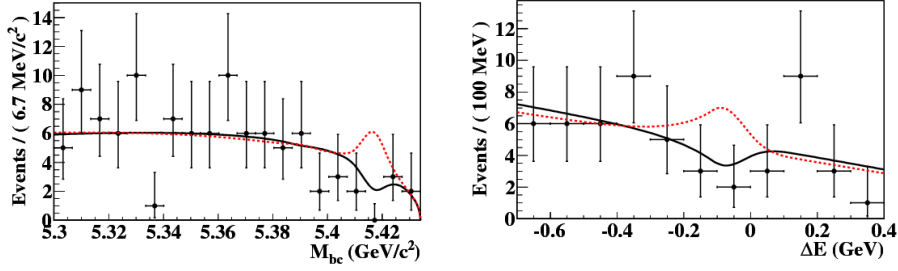


**Figure 5:** Data fits for the  $B_s^0 \rightarrow \gamma\gamma$  analysis. The projections are shown only for events inside the  $B_s^*\bar{B}_s^*$  signal region except for the plotted variable. The  $B_s^*\bar{B}_s^*$  signal region is defined as  $M_{bc} > 5.4 \text{ GeV}/c^2$  and  $-0.3 \text{ GeV} < \Delta E < 0.05 \text{ GeV}$ . The points with error bars represent the data, the solid black curve represents the total fit function, the red dashed (blue dotted) curve represents the signal (continuum background) contribution.

## Acknowledgements

The author thanks the organizers of XIII International Conference on Heavy Quarks and Leptons for excellent hospitality and for assembling a nice scientific program. This work is supported by the U.S. Department of Energy.

## References

- [1] K. A. Olive *et al.* (Particle Data Group), *Chin. Phys. C* **38**, 090001 (2014).
- [2] Unless stated otherwise, charge-conjugate modes are implicitly included.

- [3] C. H. Chen, Phys. Lett. B **520**, 33 (2001); A. R. Williamson and J. Zupan, Phys. Rev. D **74**, 014003 (2006); A. Ali, G. Kramer, Y. Li, C. D. Lu, Y. L. Shen, W. Wang and Y. M. Wang, Phys. Rev. D **76**, 074018 (2007); C. K. Chua, Phys. Rev. D **78**, 076002 (2008); K. Wang and G. Zhu, Phys. Rev. D **88**, 014043 (2013); J. J. Wang, D. T. Lin, W. Sun, Z. J. Ji, S. Cheng and Z. J. Xiao, Phys. Rev. D **89**, 074046 (2014); Q. Chang, J. Sun, Y. Yang and X. Li, Phys. Lett. B **740**, 56 (2015); H. Y. Cheng, C. W. Chiang and A. L. Kuo, Phys. Rev. D **91**, 014011 (2015).
- [4] Q. Chang, X. Q. Li and Y. D. Yang, J. Phys. G **41**, 105002 (2014).
- [5] S. Baek, D. London, J. Matias and J. Virto, J. High Energy Phys. **12**, (2006) 019; A. Hayakawa, Y. Shimizu, M. Tanimoto and K. Yamamoto, Prog. Theor. Exp. Phys. **2014**, 023B04 (2014).
- [6] C.-C. Peng *et al.* (Belle Collaboration), Phys. Rev. D **82**, 072007 (2010).
- [7] C. Oswald *et al.* (Belle Collaboration), Phys. Rev. D **92**, 072013 (2015)
- [8] S. Esen *et al.* (Belle Collaboration), Phys. Rev. D **87**, 031101(R) (2013).
- [9] B. Pal *et al.* (Belle Collaboration), Phys. Rev. Lett. **116**, 161801 (2016).
- [10] T. Abe *et al.* (Belle II Collaboration), “Belle II Technical Design Report,” arXiv:1011.0352.
- [11] J. Wicht *et al.* (Belle Collaboration), Phys. Rev. Lett. **100**, 121801 (2008).
- [12] L. Reina, G. Ricciardi and A. Soni, Phys. Rev. D **56**, 5805 (1997); S. W. Bosch and G. Buchalla, JHEP **0208**, 054 (2002); R. Mohanta and A. K. Giri, Phys. Rev. D **85**, 014008 (2012).
- [13] A. Gemintern, S. Bar-Shalom and G. Eilam, Phys. Rev. D **70**, 035008 (2004).
- [14] D. Dutta *et al.* (Belle Collaboration), Phys. Rev. D **91**, 011101 (2015).
- [15] R. Aaij *et al.* (LHCb Collaboration), Nucl. Phys. B **867**, 1 (2013).